J. Geod. Sci. 2017; 7:84–93 DE GRUYTER OPEN

Research Article Open Access

H. Jamil, M. Kadir*, R. Forsberg, A. Olesen, M. N. Isa, S. Rasidi, A. Mohamed, Z. Chihat, E. Nielsen, F. Majid, K. Talib, and S. Aman

Airborne geoid mapping of land and sea areas of East Malaysia

DOI 10.1515/jogs-2017-0010
Received March 11, 2016; accepted May 19, 2017

Abstract: This paper describes the development of a new geoid-based vertical datum from airborne gravity data, by the Department of Survey and Mapping Malaysia, on land and in the South China Sea out of the coast of East Malaysia region, covering an area of about 610,000 square kilometres. More than 107,000 km flight line of airborne gravity data over land and marine areas of East Malaysia has been combined to provide a seamless land-to-sea gravity field coverage; with an estimated accuracy of better than 2.0 mGal. The iMAR-IMU processed gravity anomaly data has been used during a 2014-2016 airborne survey to extend a composite gravity solution across a number of minor gaps on selected lines, using a draping technique. The geoid computations were all done with the GRAVSOFT suite of programs from DTU-Space. EGM2008 augmented with GOCE spherical harmonic model has been used to spherical harmonic degree N = 720. The gravimetric geoid first was tied at one tide-gauge (in Kota Kinabalu, KK2019) to produce a fitted geoid, my_geoid2017_fit_kk. The fitted geoid was offset from the gravimetric geoid by +0.852 m, based on the comparison at the tide-gauge benchmark KK2019. Consequently, orthometric height at the six other tide gauge stations was computed from $H^{GPS\ Lev} = h^{GPS} - N^{my\_geoid2017\_fit\_kk}$. Comparison of the conventional (H^{Lev}) and GPS-levelling heights ($H^{GPS\ Lev}$) at the six tide gauge locations indicate RMS height difference of 2.6 cm. The final gravimetric geoid was fitted to the seven tide gauge stations and is known as my_geoid2017_fit_east. The accuracy of the gravimetric geoid is estimated to be better than 5 cm across most of East Malaysia land and marine areas.

Keywords: Airborne gravimetry; East Malaysia; geoid modelling; seamless vertical datum

1 Introduction

Airborne gravimetry is an effective tool for mapping local gravity fields using a combination of airborne sensors, aircraft and positioning systems. It is suitable for gravity surveys over difficult terrains and areas mixed with land and ocean. Major advances in airborne scalar gravimetry, as a production system and with its detailed error models, made it possible to use airborne gravimetry as a relatively standard technique in geodesy/geophysics, with best accuracies around 1–2 mGal at 5 km resolution for fixed-wing aircraft (Forsberg et al., 1999 and Olesen et al., 2007).

The country of Malaysia consists of Peninsular Malaysia, which is part of mainland Southeast Asia, and the states of Sabah and Sarawak (East Malaysia) on the northern edges of the island of Borneo. The two distinctive parts of Malaysia, separated from each other by the South China Sea, share a largely similar landscape as both Peninsular and East Malaysia feature coastal plains rising to hills and mountains. Surface gravity data coverage in Malaysia is very sparse, mainly along the coastal plains and with varying accuracy. In 2002-2003, the Department of Survey and Mapping Malaysia (DSMM) in collaboration with Kort & Matrikelstyrensen (KMS), Denmark, has embarked on airborne gravity surveys over land areas of Peninsular and East Malaysia with a total of about 100,000 km-line gravity data was acquired (DSMM,2003). The computed gravimetric geoid (MyGeoid) over land areas of Malaysia indicate a relative accuracy of about 5 cm and has been widely adopted in GPS levelling applications. The Malaysian airborne geoid project has served as an

*Corresponding Author: M. Kadir: Info-Geomatik, No. 72, Jalan Pendidikan 4, 81300 Skudai, Taman Universiti, Johor, Malaysia, E-mail: igeom2006@gmail.com

H. Jamil, M. N. Isa, S. Rasidi, A. Mohamed, Z. Chihat: Department of Survey and Mapping Malaysia, Jalan Semarak, 50578 Kuala Lumpur, Malaysia

F. Majid: Info-Geomatik, 72 Jalan Pendidikan 4, 81300 Skudai, Taman Universiti, Johor, Malaysia

R. Forsberg, A. Olesen, E. Nielsen: DTU-Space, National Space Institute, Elektrovej, DK-2800 Kgs. Lyngby, Denmark

K. Talib, S. Aman: Faculty of Architecture, Planning and Surveying, Universiti Teknologi MARA, 40450 Shah Alam, Selangor, Malaysia

important first attempt at securing a nationwide, systematic high-accuracy country wide geoid model, providing an inspiration for other regions of the world, especially with inaccessible regions like the interior of Sarawak and Sabah.

In recent years, there has been a growing awareness of the fragile ecosystems that exists in our coastal zones and the requirement to manage our marine spaces in a more structured and sustainable manner. The challenge is to provide seamless spatial data across the land/sea interface. A major impediment is the lack of a consistent vertical datum across the land/sea interface. This paper describes the development of a new seamless geoid-based vertical datum from airborne gravity data on land and in the South China Sea out of the coast of East Malaysia region, covering an area of about 610,000 square kilometres (see Fig. 1). This new seamless land/sea vertical datum will further enhance marine cadastre and coastal geographic information system (GIS) activities in Malaysia which are vital for the understanding of many of the issues affecting the oceans and coasts, especially within the context of global warming.

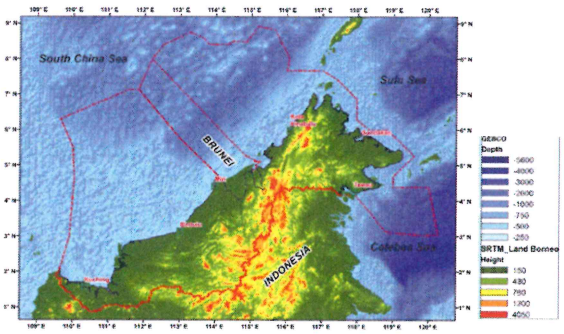

Figure 1: Land and sea areas of East Malaysia. Topographic height and seabed depth in meters.

2 Airborne gravity survey in East Malaysia

2.1 Airborne survey campaigns

The present project makes use of a stabilised two axes platform system comprises of the LaCoste & Romberg (LCR S-99) Air-Sea gravimeter and iMAR strap-down Inertial Measurement Unit (iMAR-IMU). This airborne gravimetry configuration combines two measurement systems to estimate the gravity field. Total acceleration of the aircraft is measured by a gravimeter or an IMU. Accelerations due to the movement of the aircraft are measured with signals from dual-frequency GPS receivers. The difference of these two acceleration measurements is the effect of the gravity field. As the aircraft travels, a time series of geo-referenced gravity estimates results. Lower flight speeds lead to higher resolution gravity field estimates. Herein, the resolution is defined as the minimum recoverable half wavelength. To minimise attenuation of the gravity signal, flight heights are kept low as well.

Airborne gravity surveys in East Malaysia was carried out by DSMM on-land in conjunction with MyGeoid Project in 2002-2003 (DSMM, 2003). Additional airborne surveys in the South China Sea out of the coast Malaysia - Borneo in the Sabah and Sarawak region was carried out in 2014-2016 to support the Marine Geodetic Infrastructure Project (MAGIC) (DSMM, 2017). The combined land and marine airborne gravity dataset of more than 107,000 km-flight-line in DSMM gravity database provide a seamless land-to-sea gravity field coverage in the East Malaysia area. The aircraft used in this project - Antonov-38 aircraft (on-land) and Beechcraft-BE200 aircraft (marine area) have good auto-pilot and low phugoid dynamics and have proven to be suitable for airborne gravity data acquisition. The summary of the airborne gravity survey undertaken by DSMM is described in Table 1 and Fig. 2. Over the land and territorial waters (up to 12 nautical miles - NM) flight line spacing is maintained at 5 km, while beyond the territorial waters (>12 NM) flight line spacing was at 10 km. The aircraft altitude was maintained at 2000 m, wherever possible, with a flight speed of 300 km/hr.

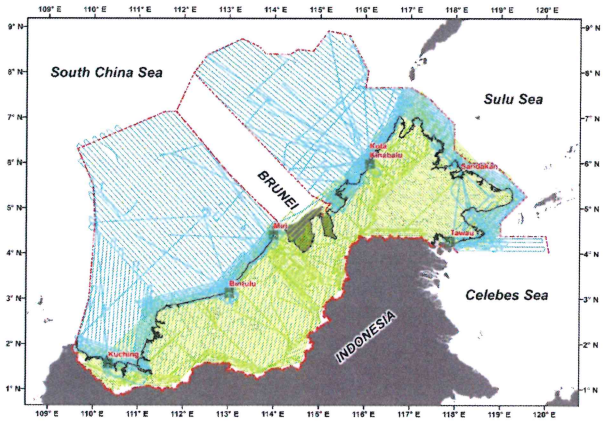

Figure 2: Airborne gravity survey of East Malaysia (green and blue lines indicate airborne survey over land and marine areas, respectively).

Table 1: Airborne gravity survey campaigns in East Malaysia

Project/Year	Airborne gravity survey coverage	Aircraft type	Airborne gravity/IMU equipment	survey (km line)	Data line spacing (km)
MyGeoid (2002-2003)	Land area	Antonov-38	LC&R S-93 and S-99 /Honeywell H764G IMU	57,000	5 km
MAGIC (2014-2016)	Marine area	BE200 (Sabah Air Aviation)	LC&R S-99 /iMAR-IMU -	50,000	5 km for <12 NM 10 km for >12 NM

Apron base readings were performed each day before and after the flight in order to monitor drift of the airborne gravimeters and make a proper connection of airborne reading to the terrestrial gravity network. Apron gravity values were established by land gravity measurements using a DTU's LaCoste & Romberg G-867 gravimeter. Gravity network adjustment was done with the program gradj.exe developed at DTU, see Table 2.

Table 2: Apron gravity values in IGSN 71 system used in 2014-2016 campaigns

Station	Apron gravity (mGal)	Sigma (mGal)	Year
Kota Kinabalu Airport	978112.982	0.030	2014
Sandakan Airport	978078.457	0.037	2015
Miri Airport	978075.548	0.037	2015
Bintulu Airport	978078.316	0.035	2016
Kuching Airport	978064.778	0.034	2016
Tawau Airport	978075.467	0.036	2016

2.2 Data Processing

The fundamental equation for the free-air gravity anomaly $\Delta g(\varphi, \lambda, h)$ from relative airborne gravity measurement can be derived as follows (for GRS80 ellipsoid, unit in mGal) (Forsberg et al., 2010):

$$\begin{aligned}\Delta g(\varphi,\lambda,h) = & f_z - \partial^2 h^{GPS}/\partial t^2 + \delta g_{Eotvos} + \delta g_{tilt} - f_{zo} \\ & + g_o - \gamma_0 + 0.30877(1 - 0.00242\sin^2\varphi) \\ & (h - N_{EGM}) + 0.75x10^{-7}(h - N_{EGM})^2\end{aligned}$$

where, (φ, λ, h) are the geodetic coordinate, f_z is the total acceleration measured by a gravimeter, $\partial^2 h^{GPS}/\partial t^2$ is the non-gravitational accelerations as determined by GPS, δg_{Eotvos} is the Eotvos correction from airborne measurements, δg_{tilt} is the gravimeter platform tilt correction, f_{zo} is gravimeter base reading, g_o is apron gravity value, γ_0 is normal gravity on the ellipsoid and, N_{EGM} is the geoid height from global gravitational model.

There are two main parts in the processing of airborne gravity data. The first is to separate gravitational accelerations from kinematics aircraft accelerations. This separation process will mainly impact the resolution of the system. A proper separation of gravitational and kinematic accelerations requires a good description of the gravity sensor response. The sensor modelling developed by DTU-Space appears to exploit most of the potential of the gravity sensor used in this project, i.e., the LaCoste & Romberg (LCR) S-gravimeter. GPS related errors will also impact the separation of accelerations and routines to identify and model such errors have been developed and implemented in this project.

The second part is to keep track of the orientation of the sensors during the flight. This is crucial to the recovery of the longer wavelengths of the gravity field, and hence for the geodetic use of the data. A new algorithm for airborne gravity processing that addresses the misalignment or off-level problem has been developed by DTU (Olesen, 2003). This new approach yield almost bias-free data. The near bias free nature of the data from the DTU processing system is the underlying fact that no crossover adjustment procedures are necessary for the data reduction.

Because of the potential high amplitude in the horizontal accelerations, and the small difference between accelerations from accelerometer and GPS measurements, the computed tilt effect is quite sensitive to the numerical treatment of the data (Olesen, 2003 and Forsberg et al., 1999). Calibration factors for the accelerometers have been determined by a Fast Fourier Transform (FFT) technique, based on the frequency dependent behaviour of the platform, and similar method has also been used for the calibration of the dynamic beam scale factor (Forsberg et al., 1999).

The iMAR-IMU processed gravity anomaly data has been used during MAGIC (2014-2016) airborne survey to make a composite gravity solution across a number of minor gaps on selected lines, using a "draping" technique, where the iMAR-IMU bias across gaps are fitted to the

LCR data, using a linear interpolator across the data gap, typically of length a few minutes. The iMAR-IMU data were processed with the commercial software Inertial Explorer from Novatel. The solution is based on a Kalman filter approach that was originally developed for the inertial navigation. The Kalman filter solves for 15 state variables among which are: 3D position, velocity, attitude, gyro biases and accelerometer biases. The latter contains the gravity information. The gravity estimate from the inertial unit is used as input to the final integrated gravity processing with program AG. The data from the LaCoste & Romberg gravimeter mainly control the longer wavelengths in the final gravity solution whereas the inertial unit will define the medium to short wavelength variations. An example of the processing output is shown in Fig. 3.

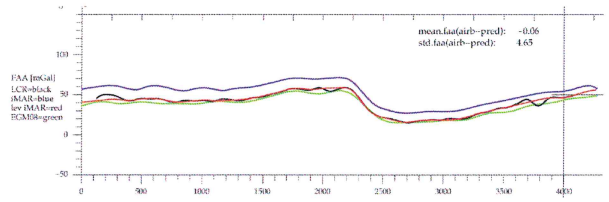

Figure 3: Combined processing of LaCoste & Romberg data and data from the inertial unit. Blue is unleveled inertial results, black is LaCoste & Romberg and red is the leveled inertial data. In green EGM08 model.

It should be pointed out that no bias adjustment on a line-by-line basis is done on the final aero-gravity data; the absolute level of the gravity line data is determined by a smoothly varying base reading curve. The aero-gravity equation is filtered with a nominal 150 sec triple-stage zero-phase forward/backward Butterworth filter, giving a resolution of about 5–7 km for the final gravity free-air anomaly data, depending on aircraft ground speed.

An altitude dependent atmospheric correction (δg_{atm}) has been applied with the equation given in Hinze et al. (2005):

$$\delta g_{atm} = 0.874 - 9.9x10^{-5}H + 3.56x10^{-9}H^2,$$

where the gravity effect is given in mGal and H is the height above sea level in meters; at aircraft altitude H =2000 m, δg_{atm} = 0.690 mGal.

The misfit in the crossing points indicates the crossover difference (root mean square, RMS). Table 3 presents the results of cross-over analysis for airborne survey campaigns of 2002-2003 and 2014-2016. This crossover error indicates the noise level on the data (un-modelled errors), assuming that the noise is uncorrelated from track to track. Weather conditions and thereby data quality has in general been good. We only encountered a few situations with more severe turbulence. The affected parts have been re-flown. Figure 4 shows the distribution of accepted gravity data and the misfit at line crossings for 2014, 2015 and 2016 surveys. RMS for the misfit in line crossings are 3.0, 2.3 and 1.9 mGal indicating a noise level of 2.1, 1.7 and 1.5 mGal for the years 2014, 2015 and 2016 respectively. These are very satisfying results and agree with results from other surveys flown under similar conditions. The reason for the lower noise in 2016 is mainly the more benign gravity field in the 2016 area, see also Fig. 6.

Table 3: Cross over analysis of the airborne survey campaigns in East Malaysia

Year	RMS crossing	Max	Line error estimate	Cross-over points
2002–2003	3.2	9.9	2.2	1311
2014	3.0	9.0	2.1	72
2015	2.3	7.1	1.7	389
2016	1.9	5.4	1.5	336

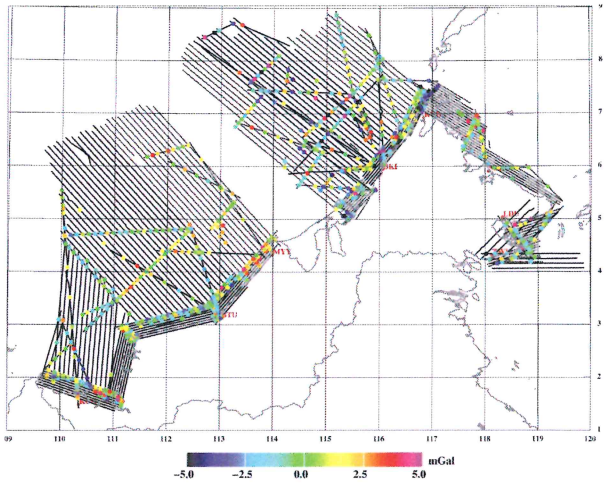

Figure 4: Crossover errors for 2014, 2015 and 2016 area

Cross over analysis also been carried out from intercomparison of the 2002-2003 airborne gravity and the 2015 airborne gravity survey in Sabah coastal areas. This comparison was done with geogrid in the DTU-Space GRAVSOFT software package (Forsberg at al., 2008), for points within 1 km distance, but separated in height. The comparison showed a result consistent with error estimate, with a mean of 1.0 mGal and RMS difference of 2.4 mGal for 394 cross-points (see Fig. 5).

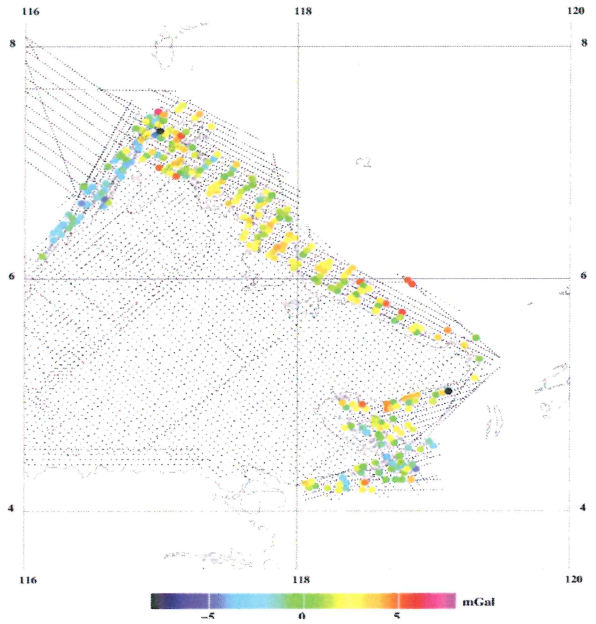

Figure 5: Cross-over errors of 2015 airborne gravity versus 2002-2003 survey.
Flight heights may differ up to 2 km or more.

2.3 Downward continuation

The downward continuation of airborne gravity and the data gridding have been performed using block-wise least-squares collocation, as implemented in the gpcol1 module of GRAVSOFT. This module uses a planar logarithmic covariance function, fitted to the reduced data. This program includes a mechanism whereby the computations can be done in blocks (e.g., 1°x 1°), extended with a border zone (e.g., 1/2°) to allow for a smooth transition between blocks. This allows for the downwards continuation of even very large data sets, where the number of linear equations to be solved would otherwise be prohibitive, should the whole downward continuation process be done in one go. In the downward continuation process by least squares collocation, the airborne gravity data represent along-track weighted averages, and the covariance functions used in the least squares collocation setup must in principle, therefore, also be similarly filtered (for details refer to Forsberg, 2002, Forsberg et al., 2007).

The airborne gravity survey database for land and marine areas of East Malaysia was compiled using ArcGIS geodatabase format. Free-air and Bouguer anomaly (density 2.67 g/cm^3) maps have been derived from the airborne data both as simple ad-hoc plots (at aircraft altitude), and as final plots from the downward continued airborne data, processed as part of the geoid determination (see Figs. 6 and 7). Data are gridded at 0.025 degrees (2.7 km) spacing. Data resolution of the filtered airborne gravity data is 5–6 km, depending on aircraft speed. Both Free-air and Bouguer anomalies have been reduced for residual terrain model (RTM) relative to a mean elevation surface. The overall results of the airborne survey are consistent and of high accuracy. Airborne gravity field also reveals many interesting regional geological features on land as well as in the marine area of Malaysia-Borneo.

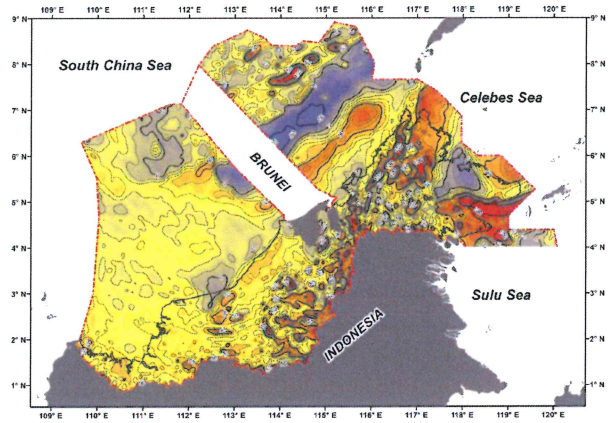

Figure 6: Downward continued Free-air gravity anomaly map in 10 mGal contours.

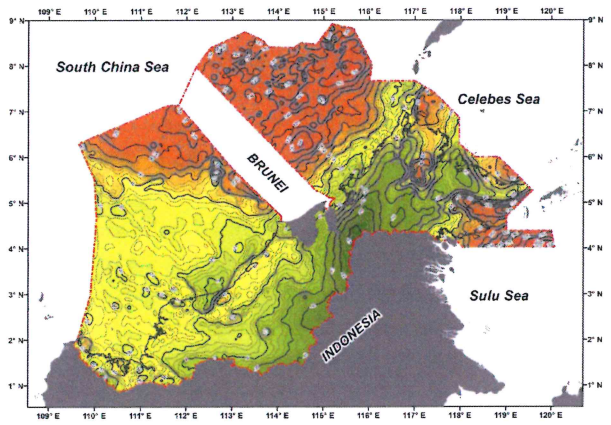

Figure 7: Bouguer gravity anomaly map in 5 mGal contours.

3 Airborne geoid modelling

3.1 Data sources

Airborne gravity data gridded at 0.025 degree (2.7 km) spacing is the main source of gravity data for the East Malaysia geoid computation. The existing surface grav-

ity data are sparsely distributed, and there are uncertainties in the gravity datum and coordinate system associated with point gravity data (Kadir, 2002). Marine gravity data from the new CryoSat-enhanced DTU-15 global marine gravity field model was used to fill gaps outside the airborne gravity survey area. EGM2008 augmented with GOCE spherical harmonic model (termed EGM08/GOCE) has been used to spherical harmonic degree N = 720, corresponding to a resolution of 15 arc-minute or approximately 28 km. The terrain part of the computations was based on the RTM method, where the topography is referred to a mean elevation level, and only terrain residuals relative to this level is taken into account (Forsberg, 1984). The mean elevation surface was derived from the SRTM 30 arc-second detailed model through a moving average filter with a resolution of approximately 45 km.

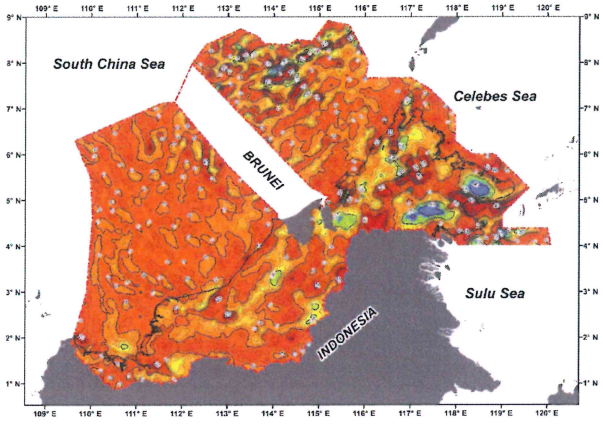

Figure 8: Residual Free-air gravity anomaly (Δg_{res}) of East Malaysia in 5 mGal contours.

3.2 Remove-restore technique

The methodology for geoid determination is based on remove-compute-restore (RCR) technique. The anomalous gravity potential T is split into three parts: $T = T_{EGM} + T_{RTM} + T_{res}$, where T_{EGM} is the anomalous gravity potential of the EGM08/GOCE global field; T_{RTM} is the anomalous gravity potential generated by RTM, i.e. the high-frequency part of the topography; T_{res} is the residual anomalous gravity potential residual, i.e. the potential corresponding to the un-modelled part of the residual gravity field. Similarly, gravity anomaly Δg also can be written in three parts: $\Delta g = \Delta g_{EGM} + \Delta g_{RTM} + \Delta g_{res}$. Following the RTM method in principle, the height anomalies ζ, i.e. the quasi-geoid, is modelled: $\zeta = T(\varphi, \lambda, H)/\gamma(\varphi, H)$, where H is the orthometric height. The quasi-geoid and the classical geoid can be viewed as "the geoid at the topography level" and the "geoid at sea-level", respectively.

The figures below illustrate the processing steps and the available data, as well as the comparisons of the different data sets to the reference fields. Table 4 shows the statistics of the original gravity data, as well as the terrain- and EGM08/GOCE-reduced data, and Table 5 comparisons to the DTU15 satellite altimetry data in the South China Sea.

Remove step: Compute the residual gravity anomaly field by subtracting the EGM08/GOCE and RTM parts from total anomalies: $\Delta g_{res} = \Delta g - \Delta g_{EGM} - \Delta g_{RTM}$. Here Δg_{res} is the residual free-air anomaly, i.e. what is left in the gravity data after the contributions of the residual terrain effect Δg_{RTM} and the global field Δg_{EGM} are subtracted (see Fig. 8).

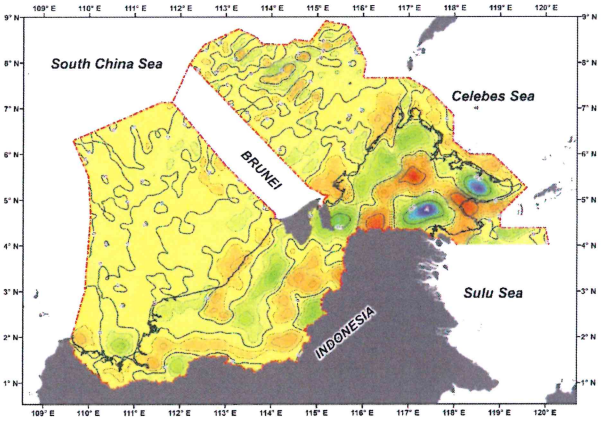

Figure 9: Computed residual height anomaly (ζ_{res}) in 0.1 m contours.

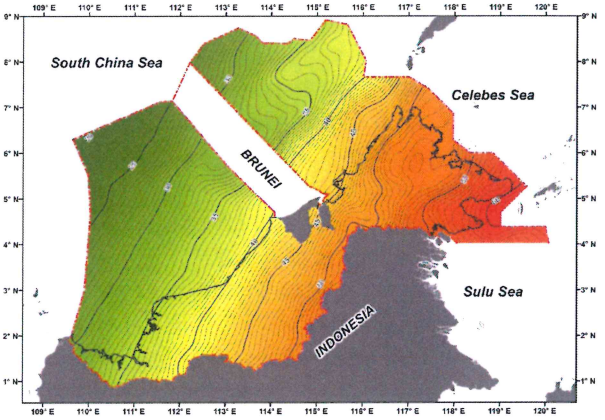

Figure 10: Add EGM08/GOCE reference geoid (ζ_{EGM}) in 0.5 m contours.

Table 4: Statistics for the original and terrain- and EGM08/GOCE-reduced data (mGal)

Gravity anomaly data	Original data Mean	Original data Std.dev.	Reduced data Mean	Reduced data Std.dev.
Airborne gravimetry 2014	18.4	22.3	0.1	8.5
Airborne gravimetry 2015	26.1	32.0	3.2	7.6
Airborne gravimetry 2016	22.9	17.0	1.9	5.8
Airborne gravimetry 2002-3	33.1	21.1	0.4	9.1
DSMM surface gravimetry	18.1	21.7	0.1	11.5
DTU-15 altimetry gravity	14.8	23.8	−0.2	6.7

Table 5: Comparisons of 2014-16 airborne gravity data to DTU15/DTU10 satellite altimetry (mGal)

Gravity anomaly data	Original data Mean	Original data Std.dev.	Difference Mean	Difference Std.dev.
Airborne gravity 2014-16	20.8	24.8	2.1	5.1
Airborne gravity 2014-16 At distance >50 km coast	15.5	24.4	−1.1	3.8
Airborne gravity minus DTU10	20.8	24.8	−1.8	5.0
DTU10 minus DTU15	N/A	N/A	0.0	2.1

Compute step: The method for the gravimetric geoid determination is spherical FFT with optimised kernels. This is a variant of the classical geoid integral ("Stokes integral"), in which there is a proper weighting of the long wavelengths from EGM08/GOCE and the shorter wavelengths from the local gravity data. Mathematically, it involves evaluation of convolution expressions of

$$\zeta_{res} = S_{ref}(\Delta\phi, \Delta\lambda) * [\Delta g_{res}(\phi, \lambda) \sin\phi]$$
$$= F^{-1}[F(S_{ref})F(\Delta g_{res} \sin\phi)]$$

Here S_{ref} is a modified "Stokes" kernel and F is the 2-dimensional Fourier transform operator. To grid the data, taking into account the varying elevations of the airborne and surface gravimetry data, block-wise least-squares collocation, using the planar logarithmic covariance model in 1° x 1° blocks with overlap, was used. For details of the geoid, determination method see Forsberg et al. (2003) or Forsberg et al. (2010), and further references therein.

The new East Malaysia gravimetric geoid my_geoid2017.gri is computed on a grid of 1.5x1.5 arc-minute resolution (corresponding to a roughly 2.7 km grid resolution). The area of computation is 0°–9°N and 99–120°E, covers a major part of the South China Sea as well, involving spherical FFT transformations in grids of 1080 x 3200 grid data points (100% zero padding).

Restore step: After residual height anomaly ζ_{res} has been computed from Δg_{res} the contribution from EGM08/GOCE (Fig. 10) and RTM (Fig. 11) are added back to get total height anomalies: $\zeta = \zeta_{EGM} + \zeta_{RTM} + \zeta_{res}$.

The relationship between geoid (N) and the quasi-geoid (ζ) is given by the approximate formula (Tziavos et al., 2013): $N - \zeta = (\Delta g_B/\gamma)H$, where Δg_B is the Bouguer anomaly and $H$is the orthometric height. This is implemented as a small correction (typically <10 cm) on a final gravimetric geoid computed from a surface data (see Fig. 12). In areas where $H = 0$, i.e. over marine areas, the quasi-geoid coincides with the geoid ($N = \zeta$). The final gravimetric geoid *my_geoid2017* is shown in Fig. 13.

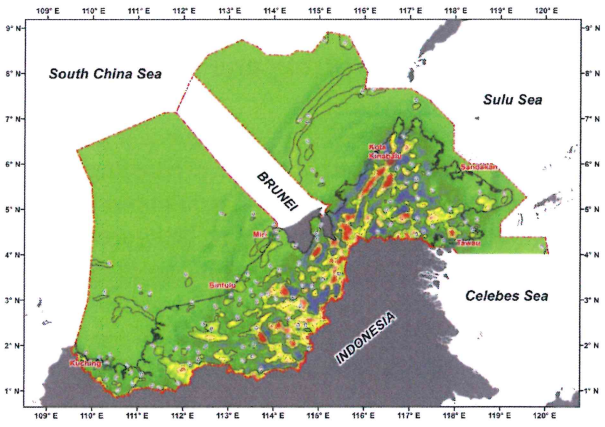

Figure 11: Add RTM geoid (ζ_{RTM}) in 0.01 m contours

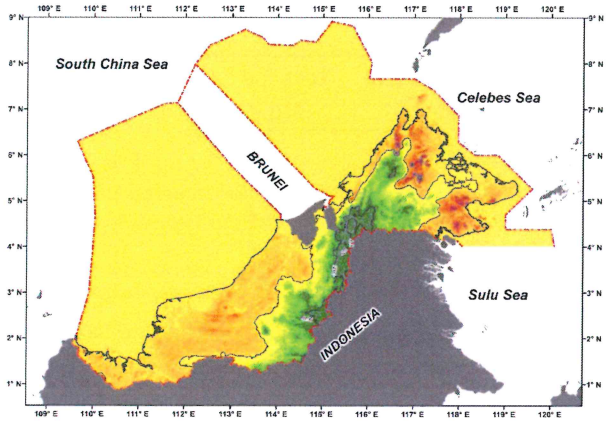

Figure 12: Add quasi-geoid to geoid correction ($N - \zeta$) in 0.01 m contours

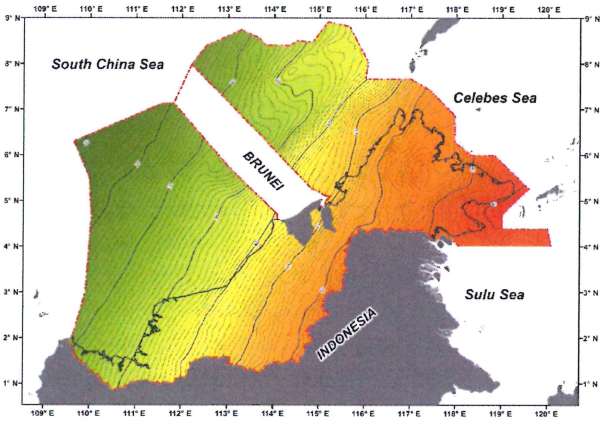

Figure 13: Final gravimetric geoid *(my_geoid2017)* of East Malaysia in 0.5 m contours

3.3 Gravimetric geoid fitting and validation

The outcome of the remove-restore technique is a gravimetric geoid, an implicit global height datum adapting the geoid to fit the local vertical datum, and to minimise possible long-wavelength geoid errors. A fitting of the geoid to GPS/tide gauge control is needed as the final geoid determination step. A GPS field campaign has been carried out in October-December 2016 at 52 locations that co-located with tide-gauges and precise levelling bench-marks (see Fig. 15). A minimum of 12 hours of GPS data was collected and subsequently processed with Novatel Waypoint software (Precise Point Positioning/precise ephemeris and baseline relative techniques) for computing the ellipsoidal height. The computed geoid height from GPS and levelling heights, $N^{GPS} = h^{GPS} - H^{Lev}$, is affected by errors from both ellipsoidal height (h^{GPS}) and conventional levelling height (H^{Lev}): $\sigma_N = \pm(\sigma_h^2 + \sigma_H^2)^{1/2}$; σ_h is estimated to be better than ±2 cm while σ_H may vary from ±2 cm to more that ±10 cm. By selecting levelling benchmarks located closest to tide gauge stations, the error in H^{Lev} can be omitted, thus the resulting error in the computed geoid N^{GPS}: $\sigma_N = \pm\sigma_h = \pm 2$ cm.

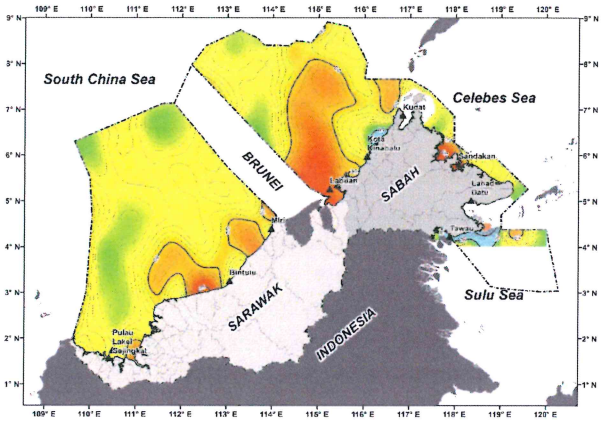

Figure 14: Mean Dynamic Topography, *MDT = DTU15/MSS - my_geoid2017_fit_kk;* in 0.01 m contours. Black triangles indicate location of tide gauge stations.

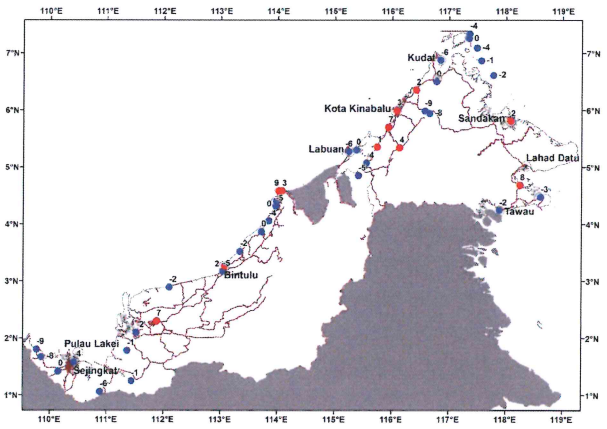

Figure 15: GPS levelling residuals $\Delta H = H^{Lev} - H^{GPS\,Lev}$ in cm at 41 GPS-levelling benchmarks

The gravimetric geoid was tied first at a one tide-gauge (in Kota Kinabalu, KK2019) to produce a fitted geoid, my_geoid2017_fit_kk. The fitted geoid was offset from the gravimetric geoid by +0.852 m: $N^{my\_geoid2017\_fit\_kk} = N^{my\_geoid2017} + 0.852$ m, based on the comparison at the tide-gauge benchmark KK2019. Consequently, orthometric heights at the six other tide gauge stations were computed from $H^{GPS\,Lev} = h^{GPS} - N^{my\_geoid2017\_fit\_kk}$. Comparison of $H^{GPS\,Lev}$ and H^{Lev} at the six tide gauge locations in-

Table 6: GPS/levelling analysis at six tide gauge locations in East Malaysia

Station ID	Nearest Tide Gauge Station	GPS Ellipsoidal Height h^{GPS} (m)	Geoid Height $N^{2017\_fit\_kk}$ (m)	Geoid Based Height $H^{GPS\,Lev}$ (m)	MSL Based Height H^{Lev} (m)	$\Delta H = H^{Lev} - H^{GPS\,Lev}$ (cm)
BM2019	Kota Kinabalu *(fitted station)*	51.855	48.222	3.633	3.633	0.0
BM205004	Kudat	52.518	49.725	2.793	2.784	−0.9
SS77	Sandakan	57.561	53.817	3.744	3.767	2.3
STDM	Tawau	60.942	57.572	3.370	3.381	1.1
K013	Kuching	37.402	34.020	3.382	3.380	−0.2
T002	Bintulu	46.148	40.775	5.373	5.428	5.5
0133	Miri	44.400	41.721	2.679	2.663	−1.6
					RMS	2.6

dicate RMS height difference of 2.6 cm (see Table 6). Also, no apparent Mean-Dynamic-Topography (MDT) is visible in the coastal areas of East Malaysia, evident in the MDT map produced from DTU15 Mean-Sea-Surface (MSS) and my_geoid2017_fit_kk (see Fig. 14).

The final geoid was then fitted to all the seven tide gauge stations and is known as my_geoid2017_fit_east. Fitting the gravimetric geoid to benchmarks closest to tide-gauge stations will not deform the gravimetric geoid as the error in the conventional levelling heights can be kept to a minimum level (see Fig. 14 for tide gauge station locations).

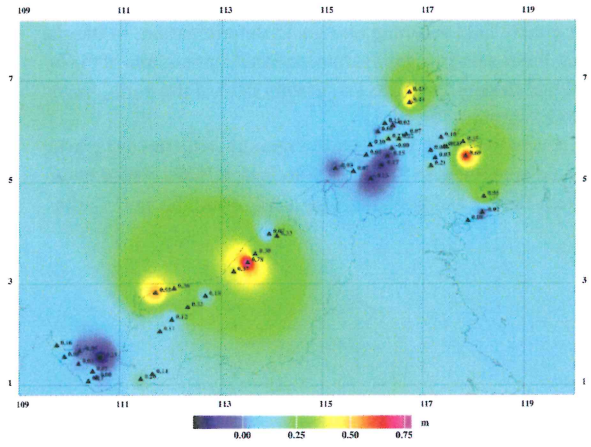

Figure 16: Fit of *my_geoid2017_fit_east* to the 2003 GPS-levelling points in East Malaysia

The final gravimetric geoid my_geoid2017_fit_east was used to validate the conventional levelling height network of the East Malaysia. Due to difficult terrain and poor accessibility in Sarawak, the levelling network is available only in the coastal areas. The new geoid was used also to transfer heights to a number of small islands off Sabah; the local H^{Lev} was determined by a short-term tide gauge measurements (few days). Figure 15 shows the differences, in cm, between the conventional and GPS-levelling heights, $\Delta H = H^{Lev} - H^{GPS\,Lev}$; height difference of more than 10 cm was not shown and interpreted as gross error in the conventional-levelling height that needs further investigations. The RMS height difference at 41 GPS-levelling benchmarks was 4.4 cm.

A comparison between the official MyGeoid_2003 and the my_geoid2017_fit_east is shown in Fig. 16. The figure shows relatively large differences, mainly due to the 2003 MyGeoid being a GPS-fitted geoid, to a data set of 300 GPS-levelling data; This indicates that the problem is the accuracy of the 2003 GPS-levelling data (likely biases in levelling).

4 Conclusions

Height reference system modernization envisages the redefinition of the vertical reference system and the realisation of a new vertical reference frame by gravimetric geoid modelling, rather than by geodetic levelling. It enables measurements of elevations, with respect to a consistent seamless vertical datum, everywhere across the country using GPS positioning.

A precise seamless land/sea gravimetric geoid model has been determined for East Malaysia using the mixed spherical harmonic model EGM08/GOCE to spherical harmonic degree N = 720, SRTM digital elevation model, DTU15 satellite altimeter-derived gravity anomalies at sea, and about 107,000 km flight line of airborne gravity data. The airborne gravity data was estimated to have an accuracy better than 2.0 mGal. The geoid computations were all done with the GRAVSOFT suite of programs from DTU-Space. The accuracy of the gravimetric geoid is estimated to be 3 to 5 cm across most of East Malaysia. The final gravimetric geoid has been fitted to seven tide gauge sta-

tions and is known as my_geoid2017_fit_east. A seamless land/sea geoid-based-height system also will further enhance the development and management of the marine environment.

Acknowledgement: We would like to record our gratitude to the Ministry of Natural Resources and Environment (NRE) Malaysia for the support given during the implementation of the Marine Geodetic Infrastructures In Malaysian Waters (MAGIC) Project.

References

Anderson O. B., 2012, Marine gravity and geoid from satellite altimetry. In Sanso F., Sideris M. G. (Ed.), Geoid Determination: Theory and Methods, pages 401-450, Springer, Berlin.

Barthelmes F., 2013, Definition of functionals of the geopotential and their calculation from spherical harmonic models. Scientific Technical Report, GeoForschungsZentrum, Potsdam, Germany.

DSMM, 2003, Airborne gravity survey and geoid determination project for Peninsular Malaysia, Sabah and Sarawak, Internal Report, Geodetic Division, Department of Survey and Mapping Malaysia.

DSMM, 2017, The Conduct of airborne gravity and magnetic survey over selected area near the international maritime boundary offshore of Sabah and Sarawak, Phase I/II (2014-2017), Internal Report, Geodetic Division, Department of Survey and Mapping Malaysia.

Forsberg R., 1984, A study of terrain corrections, density anomalies and geophysical inversion methods in gravity field modelling. OSU Report No. 355, Ohio State University, Columbus.

Forsberg R., Olesen A. V., and Keller K., 1999, Airborne gravity survey of the North Greenland continental shelf. Technical Report 10, National Survey and Cadastre (KMS), Copenhagen, Denmark.

Forsberg R., 2002, Downward continuation of airborne gravity data. Paper presented at the 3rd meeting of the International Gravity and Geoid Commission, Gravity and Geoid 2002, Thessaloniki, Greece.

Forsberg R. and Olesen A. V., 2006, Broad-band gravity field mapping by airborne gravity and GOCE. Presentation, 3rd International GOCE User Workshop, Frascati, Italy.

Forsberg R., 2007, Olesen A.V., Munkhtsetseg D. and Amarzaya A., Downward continuation and geoid determination in Mongolia form airborne and surface gravimetry and SRTM topography. In: Dergisi H. (Ed.), Proceedings of the 1st International Symposium of the International Gravity Field Service: Gravity field of the Earth, pages 259–264, Istanbul, Turkey.

Forsberg R. and Tscherning C. C., 2008, An overview manual for the GRAVSOFT Geodetic Gravity Field Modelling Programs, 2nd Edition, DTU-Space.

Forsberg R. and Olesen A. V., 2010, Airborne gravimetry. In Gouchang Xu (Ed.): Sciences of Geodesy-I, Spinger Verlag, pp. 83-104.

Hinze W. J., Aiken W., Brozena J., 2005, Coakley B. and Dater D., New standards for reducing gravity data: The North American gravity database, Geophysics, Vol. 70, No. 4.

Hofmann-Wellenhof and Moritz H., 2006, Physical Geodesy, Springer.

Kadir M., Ses S., Hisam H. and Abu S., 2002, Current and future geodetic activities in Malaysia, GNSS Forum, 17-18 May, Hong Kong.

Olesen A.V., Forsberg R., and Gidskehaug A., 1997, Airborne gravimetry using the LaCoste & Romberg gravimeter - an error analysis. In: Cannon M.E., Lachapelle G., (eds.), Proceedings of the International Symposium on Kinematic System in Geodesy, Geomatics and Navigation (KIS97), Banff, Canada.

Olesen A.V., 2003, Improved airborne scalar vector gravimetry regional gravity field mapping and geoid determination. Technical Report, National Survey and Cadastre (KMS), Copenhagen, Denmark.

Olesen A.V. and Forsberg R., 2007, Airborne scalar gravimetry for regional gravity field mapping and geoid determination. In Dergisi H. (Ed.), Proceedings of the 1st International Symposium of the International Gravity Field Service: Gravity field of the Earth, pages 277–282, Istanbul, Turkey.

Tziavos I. A. and Sideris M. G., 2013, Topography reductions in gravity and geoid modelling. In Sanso F., Sideris M. G. (Ed.), Geoid Determination: Theory and Methods, pages 337-400, Springer, Berlin.